Vietnam Journal of Agricultural Sciences

p-ISSN 2588-1299
e-ISSN 3030-4520

VJAS 2025; 8(2): 2483-2492
https://doi.org/10.31817/vjas.2025.8.2.05

# Working Parameter Optimization for Fruit Sizing Equipment with Discrete Element Simulation

**Nguyen Thi Hanh Nguyen[1], Nguyen Chung Thong[1], Duong Thanh Huan[1], Pham Thi Hang[2], Le Minh Lu[1], Nguyen Xuan Thiet [1] & Le Tien-Thinh[3,4*]**

[1]Faculty of Engineering, Vietnam National University of Agriculture, Hanoi 12400, Vietnam

[2]Faculty of Mechanical Engineering, Thuyloi University, Hanoi 11500, Vietnam

[3]Faculty of Mechanical Engineering and Mechatronics, Phenikaa School of Engineering, Phenikaa University, Yen Nghia, Ha Dong, Hanoi 12100, Vietnam

[4]PHENIKAA Research and Technology Institute (PRATI), A&A Green Phoenix Group JSC, Hanoi 11300, Vietnam

## Abstract

Despite significant progress in the field of discrete element modeling (DEM) for agricultural granular materials, currently there is little application of discrete element simulations for agricultural fruit and vegetable sorting and sizing equipment. Thus, this study employed discrete element simulation to enhance the optimization of the working parameters for spherical-shape fruit sizing equipment. The research focused on diameter sizing equipment, investigating the influence of key parameters such as the fruit moving speed and flowrate on sizing efficiency. Fifteen simulation configurations were evaluated using commercial altair EDEM software. The results revealed the optimal combinations of working parameters that maximized yield while minimizing error. This study demonstrates the potential of discrete element simulation in minimizing the need for physical prototypes, accelerating the development process, and reducing time and cost.

## Keywords

Discrete element simulation, agricultural granular materials, diameter sizing equipment, particle moving speed, particle flowrate

**Received:** November 8, 2024
**Accepted:** June 10, 2025

**Correspondence to**
Le Tien Thinh
thinh.letien@phenikaa-uni.edu.vn

**ORCID**
Le Tien Thinh
https://orcid.org/0000-0002-1603-5000

## Introduction

Size grading is a widely used process in the agricultural and food industries. For agricultural products, size grading is an important quality indicator that serves a number of purposes such as meeting quality requirements, consumer preferences, market requirements, product pricing, packaging specifications, and post-harvest processing operations requirements (Nath *et al.*, 2019). It can be seen that consumers are very concerned about the appearance quality of agricultural products. In addition, grading into uniform sizes helps in efficient packaging and transportation because uniformly sized agricultural products reduce waste and minimize the need for over-packaging, thereby reducing transportation costs and reducing environmental impacts (Coetzee, 2017). Size grading of agricultural products also allows for more efficient handling during post-harvest processing. Agricultural products of the same size can be processed together, resulting in smoother workflows and reduced processing times. Besides, uniformly sized fruits and vegetables ripen at a more consistent rate, making the ripening process easier to manage for distribution and sale. Overall, grading fruits and vegetables into different sizes improves product quality, facilitates efficient processing, and ensures that the product meets market needs and preferences. This benefits both producers and consumers, leading to a more successful and profitable fruit and vegetable supply chain.

Among the standards of size, weight, shape, color, and quality, fruit size is a very important and widely used parameter (Coetzee, 2017). Currently, there are many scientists and companies interested in developing equipment to classify agricultural fruits and vegetables by size (Van Zeebroeck *et al.*, 2006b). It should be noted that there are different shapes for fruits including spherical shapes such as apples, plums, oranges, and lemons; cone shape like carrots; cylindrical shapes like cucumbers and pineapples; and special forms such as pears and mangoes. Consequently, depending on the shape of agricultural fruits and vegetables, many classification principles have been developed (Van Zeebroeck *et al.*, 2006b). However, each working principle exhibits different advantages and disadvantages (Romuli *et al.*, 2017).

In Vietnam, several research experiments have been conducted for sizing equipment of fruits and vegetables. For instance, Huynh *et al.* (2020) estimated the mass and/or volume of agricultural fruits with asymmetrical shapes (carrots and cucumbers) by mounting a single camera on the ceiling of an imaging chamber. The carrot's weight estimation error was 95%, whereas the cucumber's was 96.7%. Also using a vision system, Tran *et al.* (2023) captured top-view images and then estimated the physical characteristics of fruits using the disc and conical frustum method. With an accuracy of over 99% for both volume and mass across 300 test samples, the obtained results were extremely competitive. Next, Huynh *et al.* (2022) integrated machine learning classifiers together with a vision system, such as K-nearest neighbor, support vector machine, decision tree, random forest, and multilayer perceptron. The authors were able to successfully select the most important features for fruit recognition from the images. Last but not least, Huynh *et al.* (2024) developed mechanical conveyor chains and object sorting automation with an Internet of Things system. With a 90% sorting accuracy, this system identified and arranged fruits including bananas, avocados, tangerines, apples, oranges, and lemons. However, all of the above mentioned research papers in Vietnam were based mainly on camera systems. There has been, until now, no research using discrete element modeling (DEM) for the development of fruit sizing equipment in Vietnam.

Most recently, discrete element modeling (DEM) has become a very promising numerical approach for investigating the interaction between agricultural granular materials (vegetables and fruits) and equipment (Li *et al.*, 2023). For instance, Xie *et al.* (2024) developed a new type of swing separation sieve for potatoes using the DEM approach. Kafashan *et al.* (2021) used the DEM technique to analyze the dynamics of apples under physical impact. In a series of studies, Van Zeebroeck *et al.* (2006b; 2006a; 2008) tried to model the damage of fruits during transport and handling employing DEM, including a case study for the vibration damage of apples. Additionally, Ghodki & Goswami (2017) investigated the flow characteristics of black pepper seeds in a cryogenic grinding system while Kanakabandi & Goswami (2019) determined their microscopic parameters for DEM simulations. In terms of citrus fruits, Wang *et al.* (2020) modeled their stalks by using DEM simulations. For rice grains, Yuan *et al.* (2022) analyzed their vibrating behavior using EDEM software.

Although DEM simulation is an already established computational technique, its application in specific local contexts remains underexplored. In Vietnam, the agricultural sector plays a crucial role in the national economy, with a growing need for efficient, mechanized solutions for post-harvest processing. However, the development of sorting equipment for agricultural products is often constrained by a lack of validated models and high prototype development costs. By employing DEM in the early design stages, researchers and engineers can simulate the behavior of particles (fruits and vegetables) under various operational conditions—such as free-fall, vibration, rotation, and impact—without immediately resorting to costly physical trials.

Despite significant progress in the field of discrete element modeling for agricultural granular materials, currently there is not much application of discrete element simulations for agricultural fruit and vegetable sorting and sizing equipment. It should be noted that simulations can be applied to minimize the experimental testing process ("prototypes"), which would be very expensive in terms of cost, human resources, and time. Therefore, this study applied the discrete element simulation method to optimize the working parameters of spherical-shape fruit sizing equipment.

## Materials and Methods

### Discrete element method (DEM)

The discrete element method was developed based on simulating the motion of discrete particles following Newton's laws (Coetzee, 2017). Therefore, the motions of the particles are determined through solving the translational and rotational equations of motion for individual particles. Considering a system of *N* spherical particles of different radii ranging between $R_1$ and $R_N$. The translational motion of a particle *i* with mass $m_i$ is described by:

$$m_i \frac{d^2\mathbf{r}_i}{dt^2} = \mathbf{F}_i \tag{1}$$

*where* $\mathbf{r}_i$ is the position vector of the particle and $\mathbf{F}_i$ is the total force acting on particle *I*, which includes forces from particle-particle contact and any external forces (such as gravity). The rotational motion of a particle is governed by:

$$I_i \frac{d\boldsymbol{\omega}_i}{dt} = \mathbf{T}_i \tag{2}$$

*where* $I_i$ is the moment of inertia of the particle (for a spherical particle, $I_i = \frac{2}{3} m_i R_i^2$), $\boldsymbol{\omega}_i$ is the angular velocity, and $\mathbf{T}_i$ is the total torque acting on the particle due to tangential forces at the contact points. In a DEM model, contact forces are typically modeled using springs, sliders, and friction sliders. In this study, for dry granular materials, the Hertz-Mindlin contact model (Horabik & Molenda, 2016) was employed. The Hertz-Mindlin contact model accounts for both normal and tangential contact forces as in the following.

The normal contact force $F_n$ between two particles *i* and *j* is typically modeled as:

$$F_n = k_n \delta^{3/2} \tag{3}$$

*where* $k_n$ is the normal stiffness of the contact and $\delta$ is the overlap distance between the two considered particles. This force is often damped to account for energy dissipation during collision, resulting in a modified normal force:

$$F_n = k_n \delta^{3/2} - \eta_n v_n \tag{4}$$

*where* $\eta_n$ is the normal damping coefficient and $v_n$ is the relative normal velocity of the particles at the point of contact.

On the other hand, the tangential contact force is described by incorporating Coulomb friction as:

$$F_t = -k_t \Delta s - \eta_t v_t \tag{5}$$

*where* $k_t$ is the tangential stiffness, $\Delta s$ is the incremental tangential displacement during the contact, $\eta_t$ is the tangential damping coefficient, and $v_t$ is the relative tangential velocity at the point of contact. The tangential force is limited by Coulomb's friction criterion:

$$|F_t| \le \mu F_n \tag{6}$$

*where* $\mu$ is the coefficient of sliding friction. When the tangential force reaches this limit, the particles begin to slide relative to each other. These coefficients are related to the interaction relationships between particles/particles and particles/machine parts, and are given to describe the energy loss when parts interact with each other (Le, 2022). The DEM simulation follows an iterative process where the above mentioned equations are solved for each time step. Small time steps are required to capture the dynamics of particle interactions accurately. For each time step, the software calculates overlap $\delta$ for contacting particles. It then computes the normal and tangential forces using the contact models. Finally, it updates the particle velocities and positions by integrating the equations of motion. In this study, ALTAIR EDEM (Altair, 2023) software was used for the discrete element simulations.

In addition to translation and rotation motions as previously discussed, it is important to emphasize that free-fall motion plays a significant role in the operation of the equipment. As the particles move along the sorting surface, they eventually encounter increasing gap openings. When the gap size exceeds the particle's characteristic dimension (e.g., diameter), the gravitational force becomes the dominant force, and the particle undergoes free-fall motion through the gap toward the conveyor. This transition from sliding/rolling to free-fall is critical in the sorting mechanism, as it determines the classification point of each particle.

## Materials and input parameters for the DEM simulations

In this study, the authors aimed to optimize the working parameters of sizing equipment for plum fruits. Plums with various physical and mechanical parameters were collected directly from the available literature (Esehaghbeygi *et al.*, 2013). The specific simulation parameters are indicated in **Table 1**. It is interesting to note that the shape of the fruit is very close to a sphere. Thus, a spherical shape was applied during the DEM simulations.

From a simulation standpoint, the spherical or near-spherical shape of plums aligns well with the assumptions in multi-sphere DEM modeling, simplifying the contact mechanics and reducing computational complexity. This makes plums a representative model for validating sorting equipment performance and developing design guidelines that can later be adapted for more complex shapes.

## Description of equipment and working principle

**Figure 1** shows the sizing equipment and working principle selected in the present study. When considering what fruit to use in this study, plums were selected because they are spherical fruits that have a consistent shape, which makes

**Table 1.** Specifications for the DEM

| Group | Specification | Detail | Unit |
|---|---|---|---|
| Particle | Fruit shape | Spherical | |
| | Fruit smallest diameter | 16 | mm |
| | Fruit largest diameter | 92 | mm |
| | Fruit particle size distribution | Uniform | |
| | Total mass of fruits | 1000, fixed | kg |
| Simulation setting | Finite element mesh for machine parts | Triangulation with one integration point | |
| | Gravity | 9.81 | m $s^{-2}$ |
| | Simulation time step | 1.08e-5 | s |
| | Total time | Depends on the flowrate | |
| | Contact model | Sliding friction: Hertz-Mindlin | |
| | | Rolling friction: standard | |
| Working parameters | Working parameter: fruit flow rate | Varies among [1, 3, 5, 7, 9] | kg $s^{-1}$ |
| | Working parameter: moving speed | Varies among [0.5, 1, 1.5] | m $s^{-1}$ |

them ideal for rolling separation. Unlike irregularly shaped objects, spherical fruits are more predictable in their motion. Plums were fed into the equipment from the feed chute from the previous stage (for instance a conveyor belt). The design flowrate of the equipment could be increased to 9 kg $s^{-1}$. The working principle of the sorting system shown in **Figure 1** involved feeding particles from a previous processing stage via a chute, with a defined flowrate. The particles were kept moving and the opening of the gaps increased gradually. When an opening was greater than the particle diameter, the particle fell onto the conveyor at the bottom and moved to the corresponding collection bin. The screen had varying openings arranged by width, from smaller to larger diameters (<43mm, 43-64mm, 64-85mm, and 85-106mm), enabling particles of corresponding sizes to fall through at different positions along the path. These falling particles were then collected into four designated reception bins (No. 1-4), aligned below the screen. To change the sorting size, the position of the compartments and bins along the length of the equipment could simply be rearranged. It should be noted that the guided vanes were positioned in the feed chute (see **Figure 1**), making the motion of the particles easier.

By feeding the fruits through a chute and keeping them in motion, the equipment could handle a large flowrate (up to 9 kg $s^{-1}$). The design allowed for the gap size to gradually increase along the length of the equipment, enabling fruits of different sizes to fall through the gaps that corresponded to their diameters. Since spherical fruits like plums roll easily and tend to remain oriented similarly under motion, they interacted well with the graded openings, ensuring consistent sorting accuracy. As the fruits dropped through the openings only slightly larger than their diameters, the equipment avoided harsh handling and reduced the risk of bruising, which is particularly important for delicate produce like plums.

## Parametric study for the working parameters

In order to deduce the most appropriate working parameters of the equipment, parametric studies were conducted. **Table 2** describes the 15 cases studied in this work by varying two control parameters: the moving speed in the range of [0.5, 1.0, 1.5] m $s^{-1}$ and the flowrate in the range

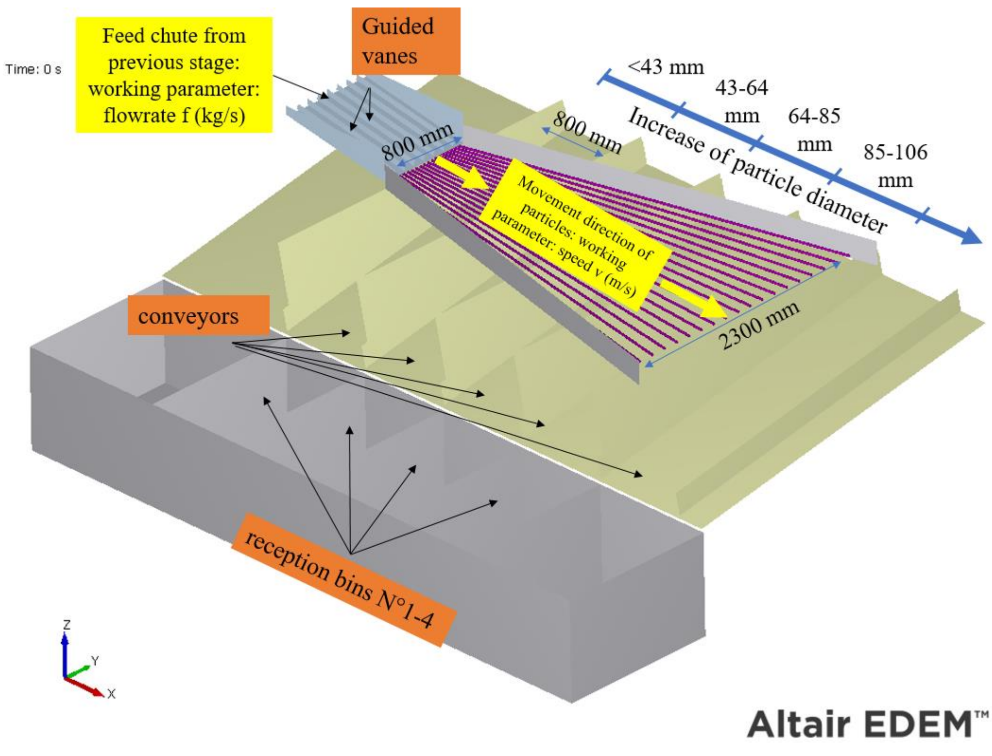


**Figure 1.** Schematic diagram of the working principle and related parts

**Table 2.** Descriptions of the cases studied.

| No. | Coding | Moving speed v (m $s^{-1}$) | Flowrate f (kg $s^{-1}$) | Computational time (h) | Number of processors used |
|---|---|---|---|---|---|
| 1 | Case_v0.5_f1 | 0.5 | 1 | ~14h | 3 |
| 2 | Case_v0.5_f3 | 0.5 | 3 | ~12h | 3 |
| 3 | Case_v0.5_f5 | 0.5 | 5 | ~8h30 | 3 |
| 4 | Case_v0.5_f7 | 0.5 | 7 | ~5h30 | 3 |
| 5 | Case_v0.5_f9 | 0.5 | 9 | ~4h30 | 3 |
| 6 | Case_v1_f1 | 1 | 1 | ~14h | 3 |
| 7 | Case_v1_f3 | 1 | 3 | ~12h | 3 |
| 8 | Case_v1_f5 | 1 | 5 | ~8h30 | 3 |
| 9 | Case_v1_f7 | 1 | 7 | ~5h30 | 3 |
| 10 | Case_v1_f9 | 1 | 9 | ~4h30 | 3 |
| 11 | Case_v1.5_f1 | 1.5 | 1 | ~14h | 3 |
| 12 | Case_v1.5_f3 | 1.5 | 3 | ~12h | 3 |
| 13 | Case_v1.5_f5 | 1.5 | 5 | ~8h30 | 3 |
| 14 | Case_v1.5_f7 | 1.5 | 7 | ~5h30 | 3 |
| 15 | Case_v1.5_f9 | 1.5 | 9 | ~4h30 | 3 |

of [1, 3, 5, 7, 9] kg $s^{-1}$ (equivalent to [3.6, 10.8, 18.0, 25.2, 32.4] ton $hour^{-1}$). The cases were coded by name associating the value of the moving speed and flowrate. It should be noted that an error of <10% was the objective of the parametric studies of the current simulations.

The authors selected the moving speed in the range of [0.5, 1.0, 1.5] m $s^{-1}$ and flowrate in the range of [1, 3, 5, 7, 9] kg $s^{-1}$ in the simulation to represent a controlled and systematic evaluation of the equipment's performance under idealized conditions. The assumption of uniformly spherical particles further simplified the model, helping isolate the effects of dynamic parameters (such as the moving speed and flowrate) without the added complexity of irregular shapes or material inconsistencies. However, such idealized conditions rarely reflect real-world scenarios, where particles (such as plums or apples) often exhibit significant variability in shape, size, moisture content, and mechanical behavior. In reality, feeding is often uneven, particles may interact or cluster, and physical phenomena like bruising or elastic deformation occur, which were not captured in a simplified DEM model. Therefore, while the simulation offers valuable insights into performance trends and system behavior, its direct accuracy in predicting real-world outcomes is limited. This approach ensures that the simulation remains a useful tool for early-stage design and optimization while acknowledging the gap between ideal conditions and practical implementation.

## Results and Discussion

All the simulations were performed using a workstation CPU AMD Ryzen Threadripper 3970X 3.7GHz. The computational time and number of processors used for the simulations are indicated in **Table 2**. All 15 configurations of the simulations were conducted and the data were stored for post-treatment. It should be noted that the total processed fruit mass was fixed as 1 ton, consequently, the smaller the flowrate, the larger the computational time, as indicated in **Table 2**. **Figure 2** presents a top view capture screen for the visualization of particles and equipment during the simulation. It can be seen that smallest particles were collected in Bin N°1, whereas largest particles were collected in Bin N°4, as expected.

However, there were also errors during the sizing process: the particles with a given size did not fall into the right bin. Consequently, in order to characterize the performance of the sizing process and deduce the most appropriate working parameters (moving speed and flowrate), sizing errors were evaluated as shown in **Figure 3**. Sizing error was calculated by dividing the number of wrong particles from the number of expected particles in each bin. It is interesting to note that the most appropriate working parameters should be the those whereas the error in each bin is the smallest. Details of the errors are evaluated below.

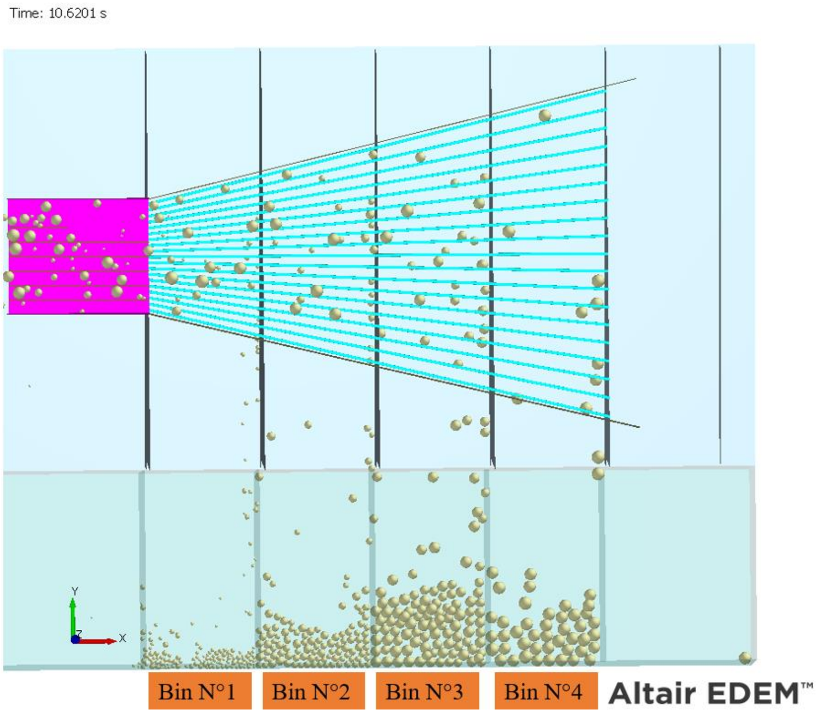


**Figure 2.** A capture screen for visualization of particles and equipment during simulation: the smallest particles were collected in Bin N°1, largest particles were collected in Bin N°4

It can be observed in **Figure 3** that there were a higher number of errors in Bins N°1, N°2, and N°3. These bins were designated for small to medium-sized particles, which were affected by dynamic behaviors such as bouncing, rolling, and shifting due to kinetic energy. Besides, it should be noted that these first bins may have been affected by insufficient settling time before reaching their intended gaps. On the other hand, Bin N°4 collected the largest particles. These particles tended to fall more directly due to gravity, with minimal influence from conveyor dynamics.

Next, **Figure 4** introduces the effect of moving speed on sizing performance via histogram distributions of the particles after finishing the process (1000kg of fruits). Three configurations of Case-v0.5-f5, Case-v1-f5, and Case-v1.5-f5 are reported. In each figure, the histograms of all the particles and of each sizing bin are shown, including the corresponding errors. It can be clearly seen that for a given flowrate of 5 kg $s^{-1}$, the error of Bin N°1 increased from 9.2% to 15.7% when the moving speed increased from 0.5 m $s^{-1}$ to 1.5 m $s^{-1}$. Similar results were also observed for the other bins. Thus, the moving speed should be 0.5 m $s^{-1}$ in order to obtain a relative small error.

Last but not least, using the moving speed of 0.5 m $s^{-1}$, **Figure 5** presents the effect of flowrate on the sizing performance via histogram distributions of the particles after finishing the process (1000kg of fruits). In each figure, the histograms of all the particles and of each sizing bin are shown, including the corresponding errors. It can be seen in Figure 5 that when using the moving speed of 0.5 m $s^{-1}$, the equipment can perform the sizing process well with a very large flowrate of 9 kg $s^{-1}$ (equivalent to 32 tons $hour^{-1}$) (see **Figure 5c**), and the maximum error was only 10.4%.

## Conclusions

This study proposed the use of the discrete particle simulations to evaluate the performance of plum fruit sizing equipment. The main conclusions drawn are as follows: (i) A spherical shape was applied for simulating the plum fruits; (ii) The moving speed should be 0.5 m $s^{-1}$ in order to obtain a relatively small error (smaller than 10%); (iii) When using the moving speed of 0.5 m $s^{-1}$, the equipment can perform the sizing

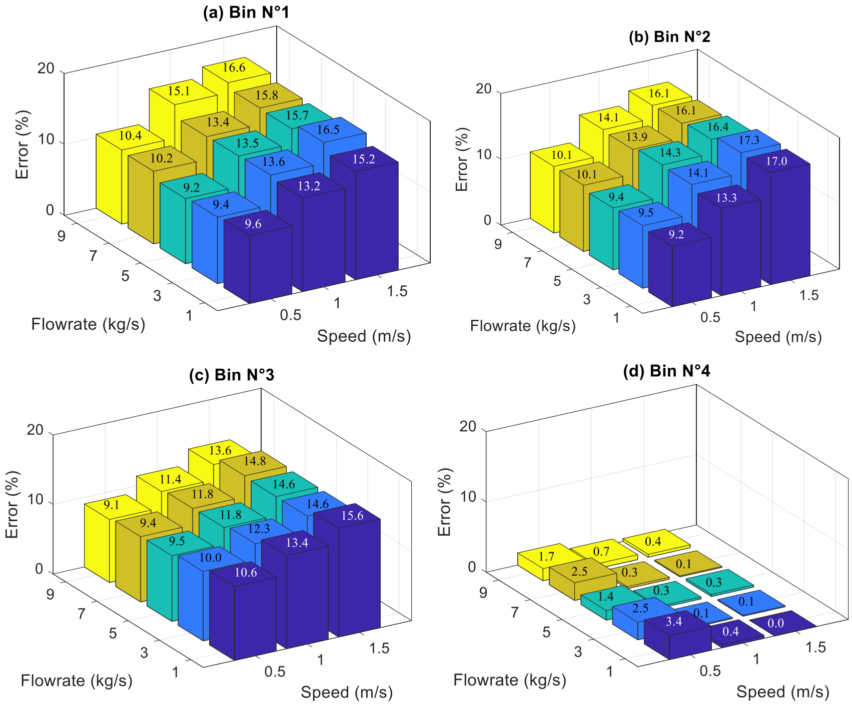


**Figure 3.** Errors of each sizing bin in varying moving speeds and flowrates (a) Bin N°1, (b) Bin N°2, (c) Bin N°3, and (d) Bin N°4

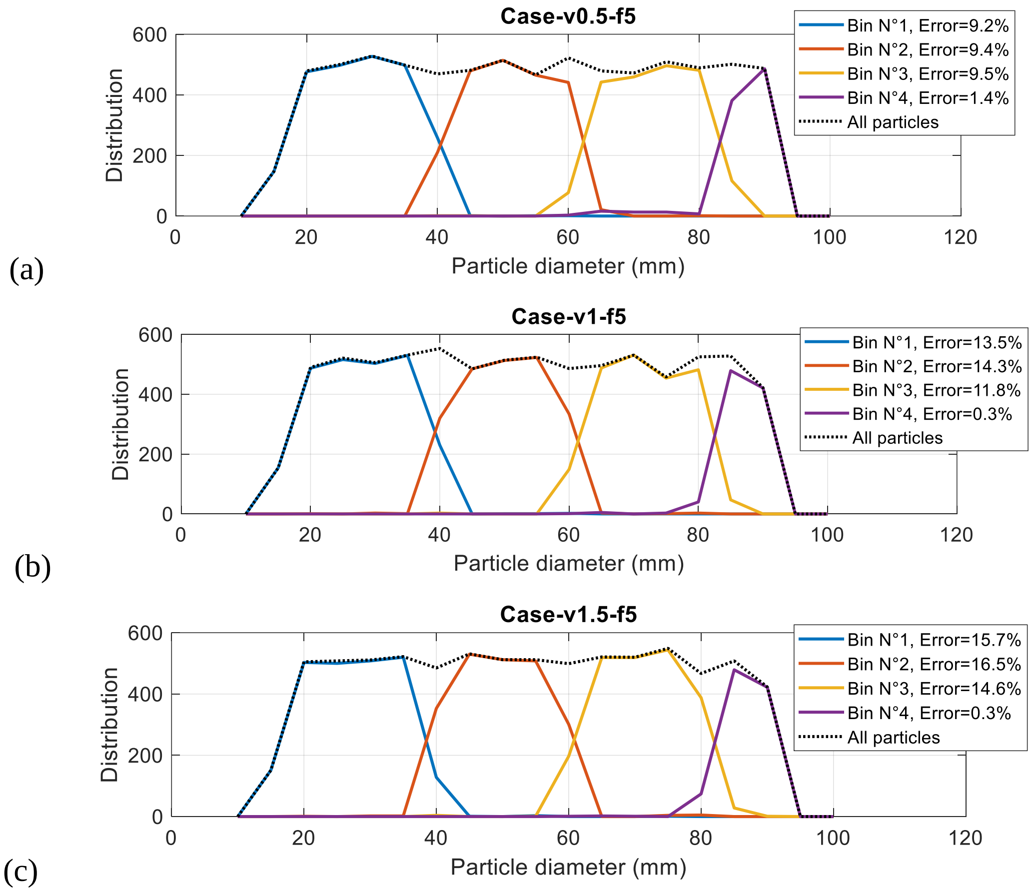


**Figure 4.** Effect of moving speed on sizing performance: histogram distributions of particles after finishing the process (1000 kg of fruits): (a) Case-v0.5-f5, (b) Case-v1-f5, and (c) Case-v1.5-f5. In each figure, the histograms of all particles and of each sizing bin are shown, including corresponding errors

process well with any flowrate smaller than 9 kg $s^{-1}$ (32.4 ton $hour^{-1}$); and (iv) DEM simulations can support the machine design process, especially in reducing experimentation, time, and cost.

However, this research needs to be developed more extensively to evaluate in detail the effects of related factors, such as increasing productivity, minimizing errors, and minimizing damage (collision, bruising, scratching). More experiments need to be performed to verify and evaluate the proposed model.

The study's findings can be extended to other Vietnamese fruits through future research. For example, by adjusting the particle shapes, sizes, mechanical properties, and motion parameters, the DEM framework can be employed to simulate the sorting of lychees, passion fruits, or even more irregularly shaped produce. Such extensions would require additional data collection (e.g., 3D scanning, mechanical testing) to accurately represent each fruit's physical behavior in simulation environments.


## Acknowledgements

This research was funded by the Ministry of Science and Technology of Vietnam under grant number ĐTĐL.CN-89/21. The authors also acknowledge the support from the Altair HyperWorks for Vietnam group.


(a)

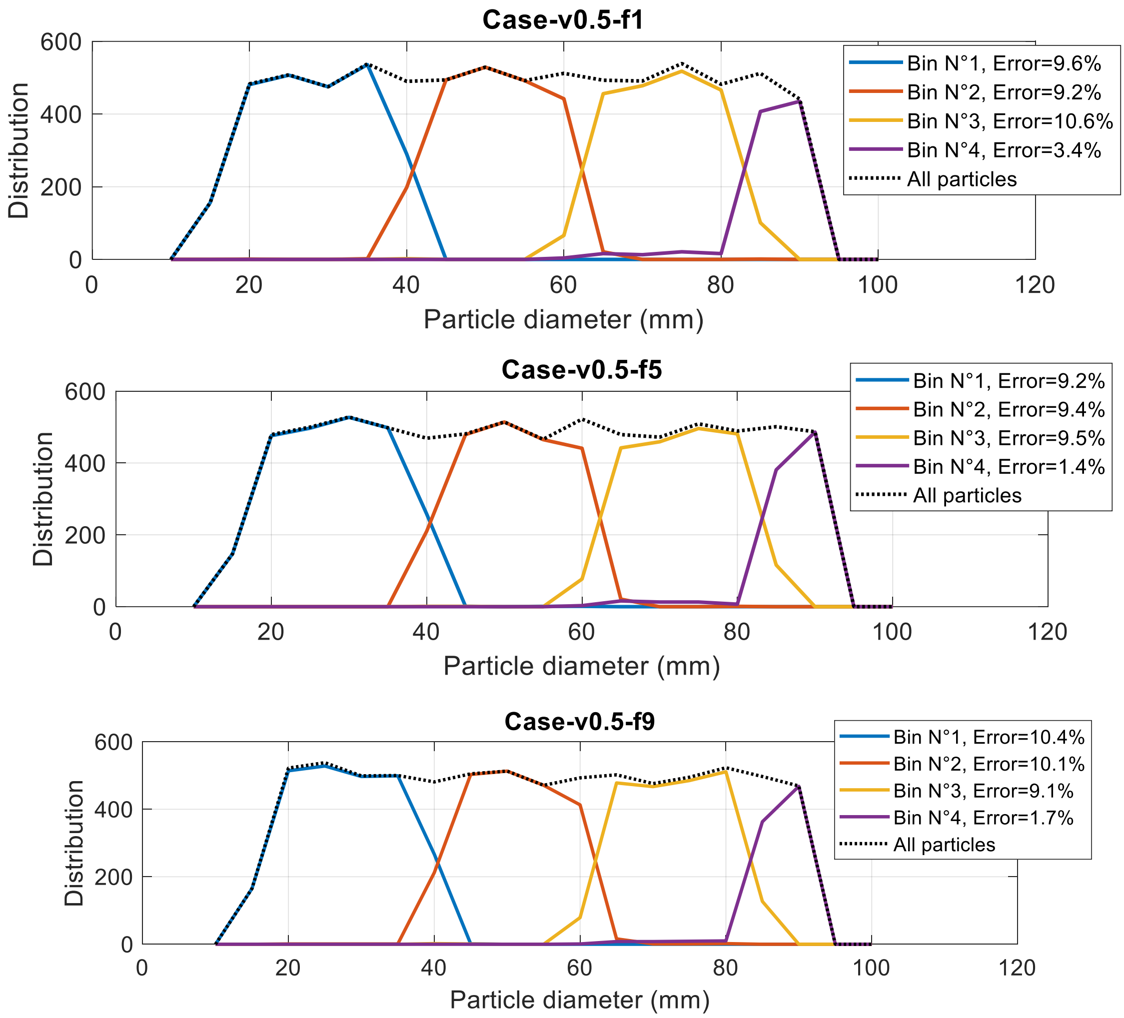


(b)

(c)

**Figure 5.** Effect of flowrate on sizing performance: histogram distributions of particles after finishing the process (1000kg of fruits): (a) Case-v0.5-f1, (b) Case-v0.5-f5 and (c) Case-v0.5-f9. In each figure, the histograms of all particles and of each sizing bin are shown, including corresponding errors

## References


Altair E. (2023). EDEM user manual. Altair Engineering Inc.

Coetzee C. J. (2017). Calibration of the discrete element method. Powder Technology. 310: 104-142.

Esehaghbeygi A., Pirnazari K., Kamali M. & Razavi J. (2013). Physical, and mechanical properties of three plum varieties (P*runus domestica* L.).

Ghodki B. M. & Goswami T. K. (2017). DEM simulation of flow of black pepper seeds in cryogenic grinding system. Journal of Food Engineering. 196: 36-51.

Horabik J. & Molenda M. (2016). Parameters and contact models for DEM simulations of agricultural granular materials: A review. Biosystems Engineering. 147: 206-225.

Huynh H. X., Lam B. H., Le H. V. C., Le T. T. & Duong-Trung N. (2024). Design of an IoT ultrasonic-vision based system for automatic fruit sorting utilizing size and color. Internet of Things. 25: 101017.

Huynh T., Tran L. & Dao S. (2020). Real-time size and mass estimation of slender axi-symmetric fruit/vegetable using a single top view image. Sensors. 20(18): 5406.

Huynh T. T. M., Le T. M., That L. T., Van Tran L. & Dao S. V. T. (2022). A two-stage feature selection approach for fruit recognition using camera images with various machine learning classifiers. IEEE Access. 10: 132260-132270.

Kafashan J., Wiacek J., Ramon H. & Mouazen A. M. (2021). Modelling and simulation of fruit drop tests by discrete element method. Biosystems Engineering. 212: 228-240.

Kanakabandi C. K. & Goswami T. K. (2019). Determination of properties of black pepper to use in discrete element modeling. Journal of Food Engineering. 246: 111-118.

Le T.-T. (2022). Investigation of force transmission, critical breakage force and relationship between micro-macroscopic behaviors of agricultural granular material in a uniaxial compaction test using discrete element method. Particulate Science and Technology. 40(5): 620-637.

Li A., Jia F., Han Y., Chen P., Wang Y., Zhang J., Hao X., Fei J., Shen S. & Feng W. (2023). Study on dynamic response mechanism of rice grains in friction rice mill and scale-up approach of parameter based on discrete element method. Innovative Food Science & Emerging Technologies. 86: 103346.

Nath S., Kumar A., Mani I., Singh J. K. & Sureja A. K. (2019). Determination of physical and mechanical properties of carrot (*Daucus carota*) for designing combine harvesting mechanism. The Indian Journal of Agricultural Sciences. 89(6): 1011-1016.

Romuli S., Karaj S. & Müller J. (2017). Discrete element method simulation of the hulling process of *Jatropha curcas* L. fruits. Biosystems Engineering. 155: 55-67.

Tran H. M., Pham K. T., Vo T. M., Le T.-H., Huynh T. T. & Dao S. V. T. (2023). A new approach for estimation of physical properties of irregular shape fruit. IEEE Access. 11: 46550-46560.

Van Zeebroeck M., Lombaert G., Dintwa E., Ramon H., Degrande G. & Tijskens E. (2008). The simulation of the impact damage to fruit during the passage of a truck over a speed bump by means of the discrete element method. Biosystems Engineering. 101(1): 58-68.

Van Zeebroeck M., Tijskens E., Dintwa E., Kafashan J., Loodts J., De Baerdemaeker J. & Ramon H. (2006a). The discrete element method (DEM) to simulate fruit impact damage during transport and handling: Case study of vibration damage during apple bulk transport. Postharvest Biology and Technology. 41(1): 92-100.

Van Zeebroeck M., Tijskens E., Dintwa E., Kafashan J., Loodts J., De Baerdemaeker J. & Ramon H. (2006b). The discrete element method (DEM) to simulate fruit impact damage during transport and handling: Model building and validation of DEM to predict bruise damage of apples. Postharvest Biology and Technology. 41(1): 85-91.

Wang Y., Zhang Y., Yang Y., Zhao H., Yang C., He Y., Wang K., Liu D. & Xu H. (2020). Discrete element modelling of citrus fruit stalks and its verification. Biosystems Engineering. 200: 400-414.

Xie S., Zhang Y., Li J. & Liu F. (2024). Analysis of Breaking and Separating Characteristics of Potato–Soil Aggregates Based on the New Type of Swing Separation Sieve. Agronomy. 14(6): 1272.

Yuan H., Liang S., Wang J. & Lu Y. (2022). Numerical Simulation and Analysis of Vibrating Rice Filling Based on EDEM Software. Agriculture. 12(12): 2013.